Int. J. Electrochem. Sci., 12 **(2017)** 10457 – 10470, doi: 10.20964/2017.11.16

International Journal of
ELECTROCHEMICAL
SCIENCE
www.electrochemsci.org

Study on S-4-methylbenzyl-O,O'-dithiophosphates as Corrosion Inhibitors for Q235 steel in HCl Solution

Chuan Lai[1,3], *Jian Wei*[3], *Xiaogang Guo*[2], *Bin Xie*[3,*], *Like Zou*[3], *Xiao Ma*[3], *Shasha Zhu*[3], *Luo Chen*[1], *Guangbing Luo*[1]

[1] School of Chemistry and Chemical Engineering, Eastern Sichuan Sub-center of National Engineering Research Center for Municipal Wastewater Treatment and Reuse, Sichuan University of Arts and Science, Dazhou 635000, PR China
[2] College of Chemistry and Chemical Engineering, Yangtze Normal University, Fuling, 408003, PR China
[3] Institute of Functional Materials, Material Corrosion and Protection Key Laboratory of Sichuan Province, Sichuan University of Science and Engineering, Zigong 643000, PR China
[*]E-mail: xiebinsuse@163.com

Received: 21 July 2017 / *Accepted:* 29 August 2017 / *Published:* 12 October 2017

Herein, S-4-methylbenzyl-O,O'-bis(4-nitrophenyl)dithiophosphate (SBOP-I) and S-4-methylbenzyl-O,O'-bis(4-t-butylphenyl)dithiophosphate (SBOP-II) were synthesized and characterized. Meanwhile, the new corrosion inhibitors for Q235 steel in HCl solution were evaluated by weight loss method and electrochemical measurements. Electrochemical measurements indicate that the inhibitors are mixed-type inhibitor, the inhibition efficiency increase with the concentration of inhibitor increase, decrease with the HCl concentration and temperature increasing. Weight loss measurement results show that the adsorption of SBOP-I and SBOP-II on Q235 steel surface obeys Langmuir isotherm, which belongs to chemical adsorption.

Keywords: Corrosion inhibitor; Electrochemical; Weight loss; Q235 steel; Langmuir.

1. INTRODUCTION

Corrosion is an afflicting problem associated with every use of metals in different industries. The use of organic inhibitors is one of the most practical methods to protect metals and alloys against corrosion, especially under the acidic environment such as using different acid solutions for cleaning, chemical decaling and pickling in industry [1-4]. It is well known that a number of organic compounds have been reported as corrosion inhibitor in acid media during the past decade and most of the effective corrosion inhibitors are organic compounds containing electronegative atoms (such as, N, P,

S and O atoms), the unsaturated bonds (such as, C=C bonds or C≡C bonds) and the plane conjugated systems including all kinds of aromatic cycles [5-8]. The corrosion inhibition of metals by reported organic inhibitors is mainly because of physical or chemical adsorption resulting from the interaction of polar centers of the inhibitor's molecule with active sites on metal surface [9-11]. As a fact, the O,O'-diaryldithiophosphates can act as the potential effective inhibitors resulting from the P, S and O atoms presence in their molecule structure. According to our previous works, the ionic compounds of the ammonium salts of O,O'-dialkyldithiophosphoric acid acting as the excellent corrosion inhibitors had been reported [12-14]. However, there are few reports about the covalence compounds of S-4-methylbenzyl-O,O'-bis(4-nitrophenyl) dithiophosphate(SBOP-I) and S-4-methylbenzyl-O,O'-bis(4-t-butylphenyl dithiophosphate (SBOP-II) as the new corrosion inhibitors.

In order to develop the new potential effective corrosion inhibitor, the aim of the present work is to investigate the corrosion inhibition of Q235 steel by SBOP-I and SBOP-I in HCl solution. Previously, the covalence compounds of SBOP-I and SBOP-II would be synthesized and characterized using by elemental analysis, FT-IR, ^{1}H, ^{13}C and ^{31}P NMR. Then, the corrosion inhibition of Q235 steel in HCl solution with different concentrations of SBOP-I and SBOP-II were evaluated by weight loss, electrochemical impedance spectroscopy (EIS) and potentiodynamic polarization measurement (Tafel). As a part of an ongoing investigation, the effects of temperature, HCl concentration and storage time on inhibition efficiency were reported.

2. MATERIALS AND METHODS

2.1 Materials

The reagents of toluene, acetone, hydrochloric acid (37%, HCl), phosphorus pentasulphide (P_2S_5), 4-t-butylphenol (4-t-BuPhOH), 4-nitrophenol (4-NO_2PhOH), dichloromethane (CH_2Cl_2), 4-methylbenzyl chloride (4-MePhCH_2Cl), diethylamine ($NHEt_2$) and sodium sulfate (Na_2SO_4) were purchased from Sinopharm Chemical Reagent Co., Ltd. All reagents were commercially available and analytically pure.

The synthesized target corrosion inhibitors of SBOP-I and SBOP-I would be characterized by elemental analysis (Carlo Erba 1106 instrument, Italy), FT-IR (Nicolet-6700 FT-IR spectrometer, 4000-400 cm^{-1}, USA), NMR (^{1}H, ^{13}C and ^{31}P, Bruker-500 NMR spectrometer, TMS as an internal standard, Germany). Meanwhile, the electrochemical measurements were employed by CHI 660D electrochemical workstation (China).

The test samples and working electrode using in this work were prepared by Q235 steel. Test samples used for weight loss measurement were cut into 5 mm×20 mm×50 mm sizes. Before testing, all of the samples were mechanically abraded with emery paper up to 1200 grit, rinsed with distilled water, degreased in acetone, and then dried at room temperature. Electrochemical measurements were conducted by conventional three-electrode system consisting of Q235 steel working electrode with an exposed area in 0.785 cm^2, a graphite electrode as counter electrode and saturated calomel electrode (SCE) as reference electrode.

The testing solution of different concentration of HCl solutions were prepared by HCl (37%, A.R.) and deionized water. During whole testing process, the temperature of the solution was controlled by DF-101S water thermostat (China), and the evaluating experiments were carried out under static conditions and open to air.

2.2 Synthesis

In order to prepare the inhibitors of S-4-methylbenzyl-O,O'-dithiophosphate derivatives, S-4-methylbenzyl-O,O'-bis(4-nitrophenyl)dithiophosphate(SBOP-I) and S-4-methyl-benzyl-O,O'-bis(4-t-butylphenyl)dithiophosphate(SBOP-II), the starting compounds of ammonium salt of O,O'-dithiophosphoric acid ($(RO)_2PS_2NH_2Et_2$) were synthesized by reaction of P_2S_5, ROH (R=4-t-BuPh and 4-NO_2Ph) with $NHEt_2$ in toluene according to reported methods [12, 14]. As $RO)_2PS_2NH_2Et_2$ prepared, the target corrosion inhibitors of SBOP-I and SBOP-II were synthesized in the following same procedure. Firstly, $(4\text{-t-BuPhO})_2PS_2NH_2Et_2$ and $(4\text{-}NO_2PhO)_2PS_2NH_2Et_2$ (10 mmol) were dissolved in CH_2Cl_2 (60 mL) in two round bottomed flask at room temperature, respectively, with that the 4-methylbenzyl chloride (10.2 mmol) was added in the solution over a period of 30 min, and the mixture was stirred about 8 hours. Afterwards, the solvent was removed under vacuum, and the residue was then taken up in 100 mL of H_2O/CH_2Cl_2 solution (1:1 v/v). The organic phase was separated and washed with 2×100 mL of H_2O, and dried over Na_2SO_4. The organic phase was purified by column chromatography (1:l CH_2Cl_2/hexane) to obtain SBOP-I and SBOP-II. After synthesized, the target synthesized corrosion inhibitors were characterized using by elemental analysis, FT-IR, ^{1}H, ^{13}C and ^{31}P NMR.

2.3 Weight loss measurement

Weight loss measurement for monitoring corrosion rate and calculating inhibition efficiency is useful because of its simple application and reliability. As the classical method for corrosion inhibition evaluating, this method were described in previous literatures [15-16]. According to this measurement, the values of corrosion rate (v, g m^{-2} h^{-1}) and corresponding inhibition efficiency (IE_W (%)) were obtained according to Eq 1 and 2, respectively. Where m_1 and m_2 are the mass of the Q235 steel samples before and after corrosion testing, Δm is average weight loss, S is the total surface area of the Q235 steel sample, t is the immersion time, v_0 and v are corrosion rate of the Q235 steel sample corrosion in HCl solution without and with different concentrations of SBOP-I and SBOP-II.

$$v = \frac{m_1 - m_2}{St} = \frac{\Delta m}{St} \quad (1)$$

$$IE_W\,(\%) = \frac{v_0 - v}{v_0} \times 100\% \quad (2)$$

2.4 Electrochemical measurements

Electrochemical measurements including potentiodynamic polarization measurement (Tafel) and electrochemical impedance spectroscopy (EIS) were conducted by conventional three-electrode system, and all potential in this study were referred to the saturated calomel electrode (SCE).

Potential sweep rate for Tafel curves was 0.5 mV s^{-1}. Corrosion current density (i_{corr}) was determined from the intercept of extrapolated cathodic and anodic Tafel lines at the corrosion potential (E_{corr}). The corresponding inhibition efficiency (IE_P (%)) based on Tafel curves were calculated as Eq (3) [17-18], where $i_{corr(inh)}$ and i_{corr} are the corrosion current density for Q235 steel in HCl solution with and without inhibitors (SBOP-I and SBOP-II).

$$IE_P\ (\%) = \frac{i_{corr} - i_{corr(inh)}}{i_{corr}} \times 100\% \quad (3)$$

EIS measurement was performed in frequency range of 100 kHz to 10 mHz using a sinusoidal AC perturbation with amplitude of 10 mV. EIS parameters were fitted by using Z-View software. Charge transfer resistance (R_{ct}) was obtained from the diameter of the semicircle of the Nyquist plot. The corresponding inhibition efficiency derived from EIS, IE_E (%), was calculated using Eq (4) [19-20], where R_{ct} and R_{ct}^0 are the values of charge transfer resistance for Q235 steel in HCl solution with and without inhibitors (SBOP-I and SBOP-II).

$$IE_E\ (\%) = \frac{R_{ct} - R_{ct}^0}{R_{ct}} \times 100\% \quad (4)$$

3. RESULTS AND DISCUSSION

3.1 Characterization

Table 1. Elemental analysis of SBOP-I and SBOP-II

Inhibitor	Molecular formula	Anal. Calcd				Anal. Found			
		C(%)	H(%)	N(%)	S(%)	C(%)	H(%)	N(%)	S(%)
SBOP-I	$C_{20}H_{17}O_6PS_2N_2$	50.42	3.57	5.88	13.45	50.40	3.59	5.87	13.43
SBOP-II	$C_{28}H_{35}O_2PS_2$	67.47	7.03	0.00	12.85	67.07	7.39	0.00	12.81

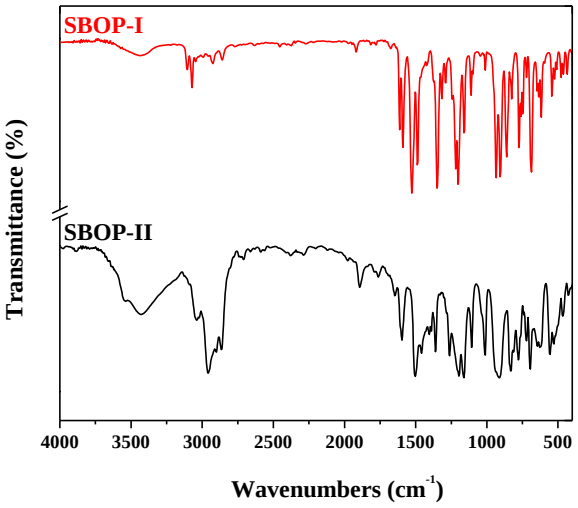

Figure 1. Infrared spectra of SBOP-I and SBOP-II

Table 2. Infrared spectra data of SBOP-I and SBOP-II (cm^{-1})

Inhibitor	ν (=C-H)	ν (C=C)	ν ((P)-O-C)	ν (P-O-(C))	ν (S-C)	ν_{asym} (PS_2)	ν_{sym} (PS_2)
SBOP-I	3071.5(w) 3105.1(w)	1526.7(s) 1589.8(s) 1613.0(m)	1159.3(m) 1201.7(s) 1218.7(s)	905.6(s) 934.7(s) 1111.3(w)	861.1(s)	617.7(m) 687.1(s) 773.9(s)	524.6(w) 542.5(w)
SBOP-II	3041.5(w)	1507.3(s) 1600.4(m)	1165.8(s) 1199.5(s) 1266.1(s)	916.1(s) 1016.2(s) 1110.6(m)	835.2(s)	631.3(m) 699.6(s) 726.0(m) 781.5(s)	533.4(m) 560.5(s)

w=weak, s=strong, m=medium.

Table 3. ^{1}H, ^{13}C and ^{31}P NMR spectra data of SBOP-II

Inhibitor	^{1}H NMR	^{13}C NMR	^{31}P NMR
SBOP-II	1.38 (s, 18H, 2C(CH_3)$_3$), 2.40 (d, *J* = 10.70Hz, 3H, CH_3) 4.27 (d, *J* =14.58 Hz, 2H, SCH_2) 6.82 -7.42 (m, 12H, 3Ph-*H*)	21.21(SCH_2), 38.91(CH_3), 39.00 (C(CH_3)$_3$), 46.38(CMe_3), 121.68, 125.77, 129.11, 129.53, 129.66, 133.17, 137.71, 150.58 (MeC_6H_4, $Me_3CC_6H_4$)	88.98 (t, *J*=14.58 Hz)

s=singlet, d=doublet, t=triplet, q=quartet.

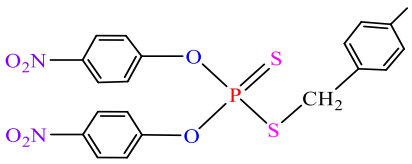

SBOP-I

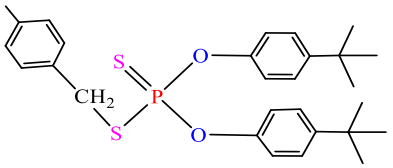

SBOP-II

Figure 2. Chemical structures of SBOP-I and SBOP-II

In order to characterize and confirm the molecular structure of target corrosion inhibitors, herein, different technologies including elemental analysis, FT-IR, ^{1}H, ^{13}C and ^{31}P NMR were employed to analyze the chemical structural of SBOP-I and SBOP-II. The characterization results of elemental analysis and NMR (^{1}H, ^{13}C and ^{31}P) were presented in Table 1 and 3, respectively. In addition, the infrared spectra and data of target corrosion inhibitors were shown in Figure 1 and Table 2.

According to the results of elemental analysis, the calculated and observed elemental analysis data for the synthesized inhibitors are in good agreement and fit well the structure of SBOP-I and SBOP-II showing in Figure 2. Meanwhile, the FT-IR, ^{1}H, ^{13}C and ^{31}P NMR results were further confirmed that the chemical structures with SBOP-I and SBOP-II.

3.2 Weight loss measurement

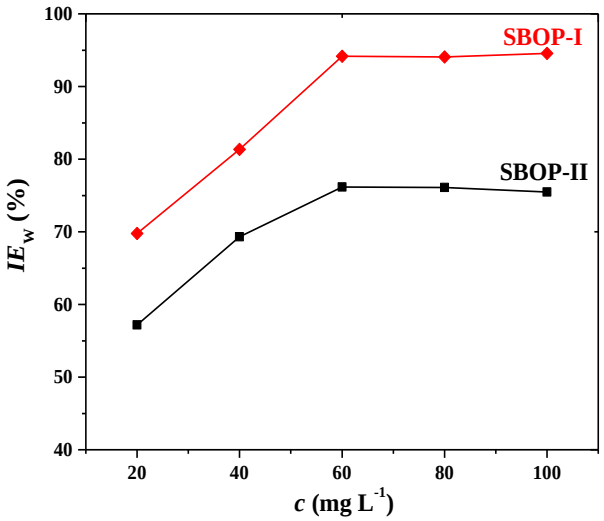

Figure 3. The inhibition efficiency for Q235 steel in 1.0 M HCl with various concentrations of SBOP-I and SBOP-II at 30 °C from weight loss measurement

In this study, the relationships between inhibitors concentration and inhibition efficiency (IE_W(%)) for Q235 steel in 1.0 M HCl at 30 °C was exhibited in Figure 3. From this figure, it can be found that the inhibition efficiencies increase with concentration of SBOP-I and SBOP-II increase, when the concentration of inhibitors increase to 60 mg L^{-1}, the inhibition efficiencies change slightly with the inhibitors concentration further increased, and a similar result had been reported in the literature [21]. This is due to the surface coverage of the inhibitors on Q235 steel surface increase with inhibitors concentration increasing. The corrosion inhibition attributed to the adsorption of components involving heteroatoms (S, P and O) and the π electron of benzene rings in inhibitors molecular on Q235 steel surface. The components can retard the dissolution of Q235 steel by blocking its active corrosion sites. The results also suggest that the inhibition efficiency of SBOP-I higher than the inhibition efficiency of SBOP-II, the difference of corrosion inhibition contribute to the different substituent (-NO_2 and –$C(CH_3)_3$) resulting from the steric and the conjugative effect of -NO_2 and –$C(CH_3)_3$. With the concentration of SBOP-I and SBOP-II increase to 80 mg L^{-1}, the inhibition efficiencies are 94.56% and 75.47%, which further demonstrate that the inhibitor of SBOP-I can act as an effective corrosion inhibitor for Q235 steel in HCl solution.

3.3 Potentiodynamic polarization measurement

Potentiodynamic polarization measurement is a rapid and convenient method for evaluating the performance of corrosion inhibition. All polarization (Tafel) curves for Q235 steel in 1.0 M HCl with various concentrations of SBOP-I and SBOP-II obtained by this method at 30 °C were presented in Figure 4 (a) and (b). Based on this measurement, the electrochemical parameters for Q235 steel corrosion in 1.0 M HCl with various concentrations of SBOP-I and SBOP-II including corrosion

potential E_{corr} (mV, vs SCE), corrosion current density i_{corr} (μA cm^{-2}), cathodic and anodic Tafel slopes β_c and β_a (mV dec^{-1}) and corresponding inhibition efficiency IE_P (%) were listed in Table 4.

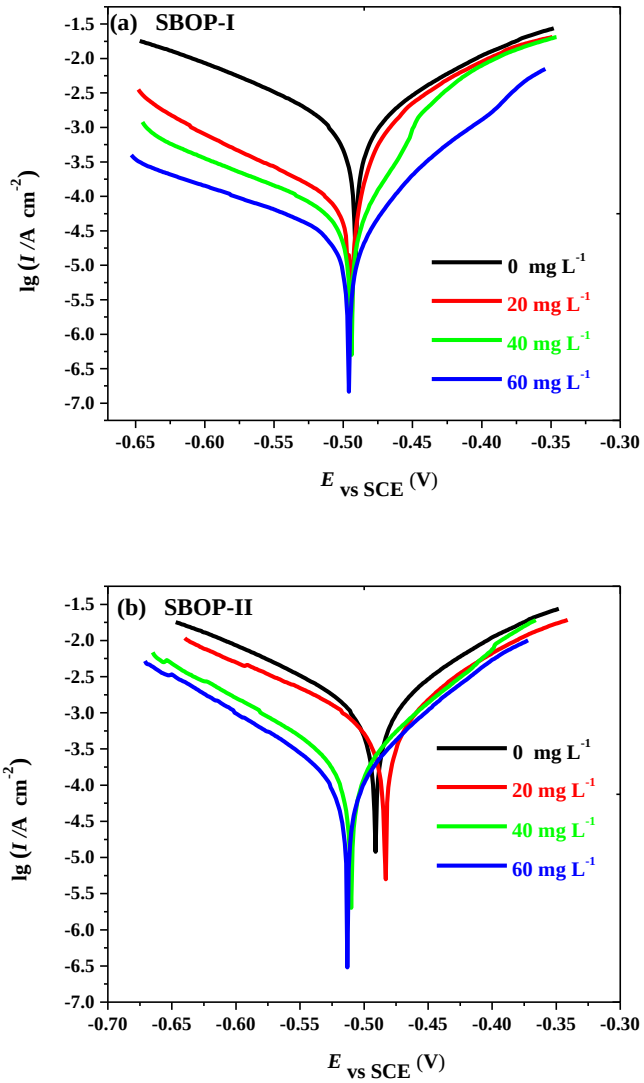

Figure 4. Polarization curves for Q235 steel in 1.0 M HCl solution with various concentrations of SBOP-I (a) and SBOP-II (b) at 30℃

According to Figure 4 (a), (b) and Table 4, it can be found that the Tafel curves are shifted to lower current regions in the presence of inhibitors, showing the inhibition tendency of studied inhibitors in 1.0 M HCl, which indicate both SBOP-I and SBOP-II can reduce the Q235 steel anodic dissolution and retard the H^+ reduction. The inhibition effect enhances with the increase of SBOP-I and SBOP-II concentration, resulting from the adsorption of inhibitors on the Q235 steel electrode surface. A possible mechanism is the adsorption of SBOP-I and SBOP-II on Q235 steel surface through the electron pair of heteroatoms (S and O) and the π electron of benzene rings, which can block the Q235 steel surface and reduces the corrosive attraction of Q235 steel in HCl media[13,14].

Apparently, from Table 4, the corrosion current density is much smaller in the presence of SBOP-I and SBOP-II comparing with that in the absence of SBOP-I and SBOP-II for Q235 steel in 1.0

M HCl, and which decrease with the inhibitor concentration increase. Inhibition efficiency increase with inhibitors concentration increasing is due to the increase of the blocked fraction of the Q235 steel electrode surface by adsorption. At the concentration of SBOP-I and SBOP-II increase to 60 mg L^{-1}, the inhibition efficiencies are 95.31% and 73.88%, respectively. The results reveal that SBOP-I can act as an effective corrosion inhibitor for Q235 steel in HCl solution. Meanwhile, it can be found that the inhibition efficiency of SBOP-II lower than SBOP-I at the same concentration, the difference between SBOP-I and SBOP-II also attributed to the different substituent on the phenyl.

Table 4. The polarization parameters and inhibition efficiencies for Q235 steel in 1.0 M HCl with various concentrations of SBOP-I and SBOP-II at 30 °C

Inhibitor	C (mg L^{-1})	E_{corr} (mV)	β_a (mV dec^{-1})	β_c (mV dec^{-1})	I_{corr} (μA cm^{-2})	IE_P (%)
Blank	0	-464	151.56	153.37	1714.65	
SBOP-I	20	-494	146.41	99.70	491.76	71.32
	40	-494	125.63	82.20	280.35	83.65
	60	-496	101.63	64.18	80.42	95.31
SBOP-II	20	-483	136.80	104.17	801.08	53.28
	40	-510	100.70	73.26	591.9	65.48
	60	-513	93.63	66.23	447.87	73.88

In addition, based on Tafel curves, the type of corrosion inhibitors can be determined [6, 22-23]. It is clearly that the corrosion potentials shift slightly in the negative direction from Table 4. Here, the shift of corrosion potential in the range of 19-49 mV suggest that SBOP-I and SBOP-II all act as the mixed-type inhibitor.

3.4 Electrochemical impedance spectroscopy

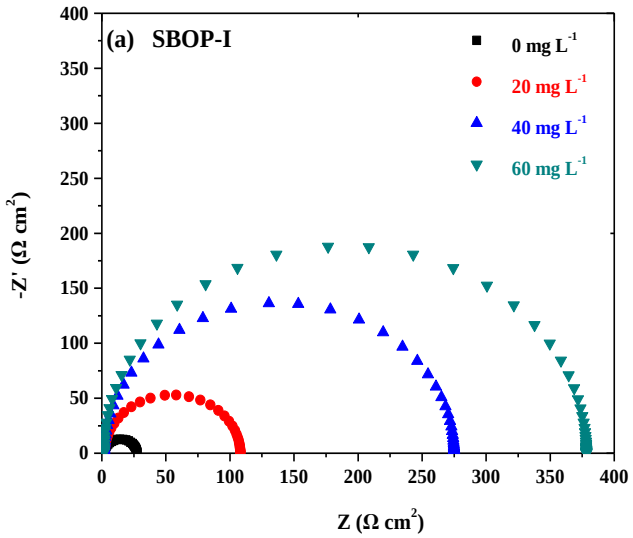

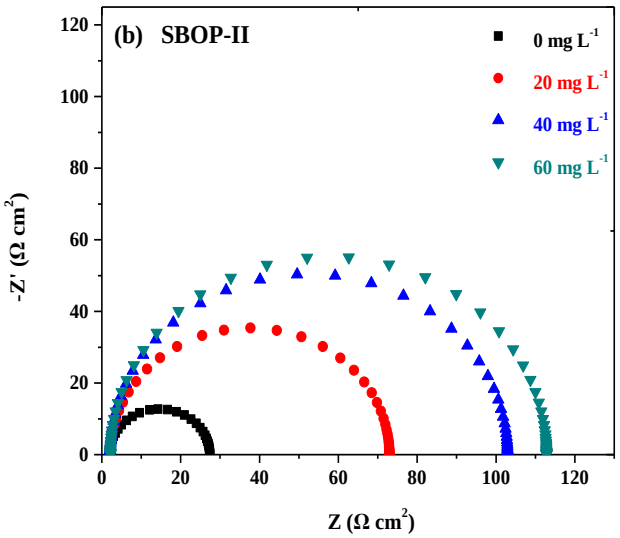

Figure 5. Nyquist diagrams for Q235 steel in 1.0 M HCl solution with various concentrations of SBOP-I (a) and SBOP-II (b) at 30℃

Figure 5 (a) and (b) show the Nyquist diagrams for Q235 steel in 1.0 M HCl with various concentrations of SBOP-I and SBOP-II at 30°Cfrom EIS. The double layer capacitance (C_{dl}), charge transfer resistance (R_{ct}) and corresponding inhibition efficiency (IE_E(%)) obtained from EIS were listed in Table 5. Based on this table, it can be found that all the Nyquist plots show a single capacitive loop, in both uninhibited (blank solution) and inhibited (HCl solution with SBOP-I and SBOP-II) solutions, which is attributed to the charge transfer of corrosion process.

Table 5. The electrochemical parameters of impedance and inhibition efficiencies for Q235 steel in 1.0 M HCl with various concentrations of SBOP-I and SBOP-II at 30 °C

Inhibitor	C (mg L^{-1})	R_p (Ω cm^{-2})	C_{dl} (μF cm^{-2})	IE_E (%)
Blank	0	25.44	78.36	—
SBOP-I	20	105.9	17.25	75.98
	40	273.1	6.33	90.68
	60	376.7	4.64	93.25
SBOP-II	20	70.76	32.9	64.05
	40	100.9	29.78	74.79
	60	110.6	24.21	77.00

The impedance spectra show that the single semicircle and the diameter of semicircle increase with the concentration of SBOP-I and SBOP-II increasing. From Table 5, it reveals that the charge transfer resistance increase and the double layer capacitance decease with the concentration of SBOP-I and SBOP-II increasing. The decrease of double layer capacitance may be due to the decrease of the local dielectric constant or the increase of the thickness of the electrical double layer, indicating that the inhibitors adsorbed on Q235 steel surface. The increase of charge transfer resistance can be

attributed to the formation of protective film on the Q235 steel/solution interface. The inhibition efficiency recorded by EIS are 93.25% and 77.00% for Q235 steel in 1.0 M HCl with 60 mg L^{-1} SBOP-I and SBOP-II. This results obtained from EIS are in good agreement with the results obtained from the other test methods including weight loss and potentiodynamic polarization measurement.

3.5 Adsorption isotherm

The adsorption isotherm can be used to analyze the interaction of the SBOP-I and SBOP-II on Q235 steel surface. Usually, both the physisorption and chemisorption as two main types of interaction are used to describe the adsorption of inhibitor on metal surface**.**

In order to confirm the reasonable adsorption isotherm for SBOP-I and SBOP-II on Q235 steel surface in HCl solution, various isotherms involving Langmuir, Frumkin, Temkin and Flory–Huggins isotherms are employed based on the data in Figure 3. The fitting results reveal that the adsorption of SBOP-I and SBOP-II on Q235 steel surface obeys Langmuir adsorption isotherm (Eq. 5) [6, 13, 24], where C is the SBOP-I and SBOP-II concentration, K_{ads} is the adsorption equilibrium constant and θ is the surface coverage. θ for various concentrations of SBOP-I and SBOP-II in 1.0 M HCl were calculated by Eq. 6 according to Eq 1.

$$\frac{C}{\theta} = \frac{1}{K_{ads}} + C \quad (5)$$

$$\theta = \frac{v_0 - v}{v_0} \quad (6)$$

The plots of C/θ versus C yield the straight lines were presented in Figure 6. The strong correlation (R^2>0.998) suggest that the adsorption of SBOP-I and SBOP-II on Q235 steel surface in 1.0 M HCl obey Langmuir adsorption isotherm. Meanwhile, the standard free energy of adsorption (ΔG^0_{ads}) can be determined from the intercepts of the straight lines using Eq. 7, where R 8.314 J K^{-1} mol^{-1} is gas constant, T (K) is absolute temperature and 55.5 (mol L^{-1}) is the molar concentration of water in the solution expressed in molarity units.

$$K_{ads} = \frac{1}{55.5} \exp\left(-\frac{\Delta G^0_{ads}}{RT}\right) \quad (7)$$

Based on Eq 7, the values of K_{ads} and ΔG^0_{ads} for SBOP-I and SBOP-II on Q235 steel were listed in Table 6. It can be found that the calculated values of ΔG^0_{ads} for SBOP-I and SBOP-II all lower than -40.00 kJ mol^{-1}, which are -43.20 and -42.71 kJ mol^{-1}, respectively. It indicates that the adsorption processes of SBOP-I and SBOP-II on Q235 steel surface in 1.0 M HCl belongs to chemical adsorption [6, 13]. Compare the ionic compounds of dialkyldithiophosphate derivative as corrosion inhibitor in H_2SO_4 solution[13,14] with the covalence compounds of SBOP-I and SBOP-II in HCl solution, according to the values of ΔG^0_{ads} , it can be found that the SBOP-I and SBOP-II on Q235 steel in HCl solution show a more prominent chemical adsorption.

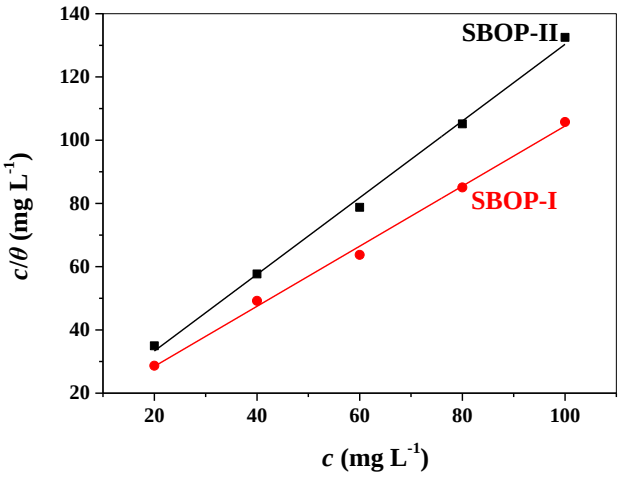

Figure 6. Langmuir adsorption isotherm for SBOP-I and SBOP-II on Q235 steel in 1.0 M HCl at 30 °C

Table 6. The adsorption parameters for SBOP-I and SBOP-II on Q235 steel in 1.0 M HCl at 30 °C

Inhibitor	Y=a+bX	ΔG^0_{ads} (kJ mol^{-1})	R^2	K_{ads} (L mol^{-1})
SBOP-I	Y=9.457+0.950X	-43.20	0.9983	5.011×10^5
SBOP-II	Y=9.066+1.212X	-42.71	0.9985	4.117×10^5

3.6 Effect of temperature, HCl concentration and storage time

The effect of temperature, HCl concentration and storage time on inhibition efficiency (IE_P(%)) from potentiodynamic polarization measurement were presented in Figure 7 (a), (b) and (c). Based on Figure 7 (a), it can be found that the inhibition efficiency decrease with temperature increasing, with temperature increase from 25℃ to 45℃ that the inhibition efficiency of SBOP-I and SBOP-II (60 mg L^{-1} in 1.0 M HCl) drop from 97.94%, 76.31% (25℃) to 91.99%, 71.97% (45℃) , respectively. The same tendency of temperature effect on inhibition efficiency was reported in the literature [12]. The decrease of inhibition efficiency and increase of corrosion is due to the increasing of inhibitor molecules desorption from Q235 steel surface.

Meanwhile, from Figure 7 (b), it is obvious that the inhibition efficiency decrease with HCl concentration increasing, and the minimum inhibition efficiency of SBOP-I and SBOP-II in 60 mg L^{-1} for Q235 steel in 5.0 M HCl at 30 °C are 53.03% and 74.84%. The decrease of the inhibition efficiency from 98.89%, 83.17% (0.1 M HCl) to 74.84%, 53.03% (5.0 M HCl) are contributed to the increase of H^+ concentration. The similar result was reported by Lu and Wei [25-26].

Additional, according to the effect of storage time on inhibition efficiency from Figure 7 (c), the inhibition efficiency slightly fluctuate with storage time changing. At 30℃, in 1.0 M HCl with 60 mg L^{-1} SBOP-I and SBOP-II after 168 hours later, the inhibition efficiency still up to 95.03% and 74.98%, respectively.

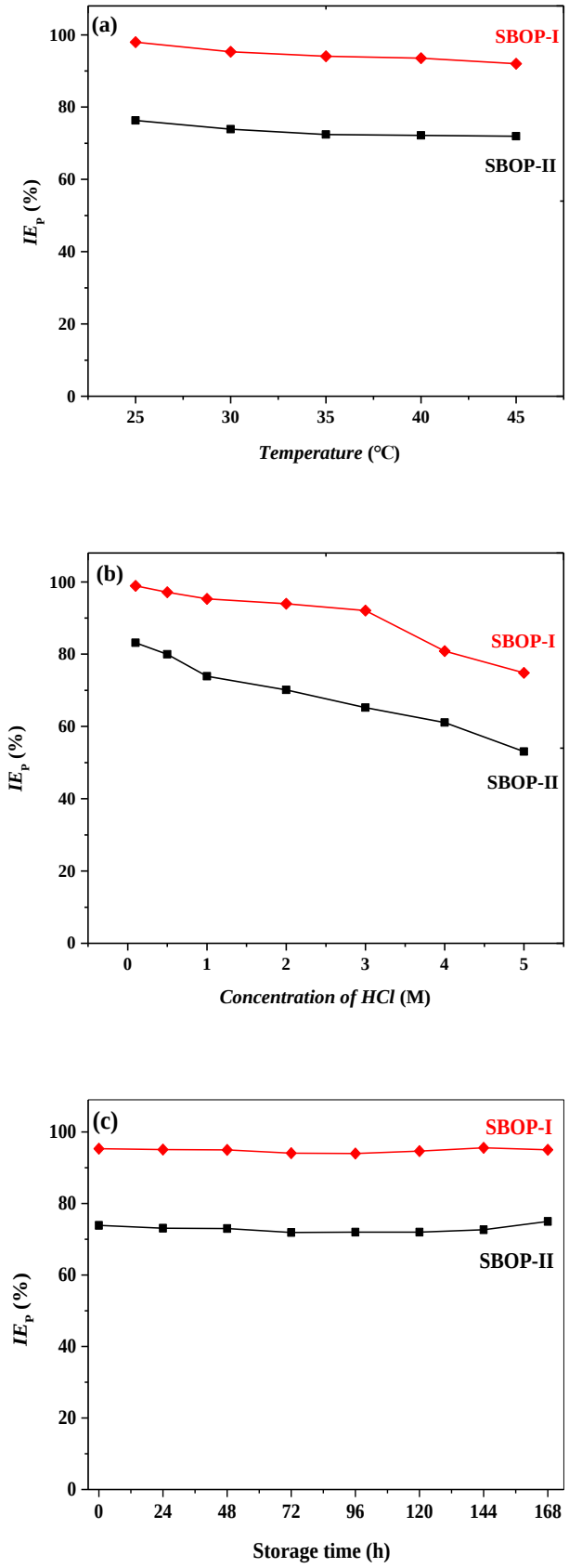

Figure 8. The influence of temperature (a), HCl concentration (b), and storage time (c) on inhibition efficiency from potentiodynamic polarization measurement

Compare the ionic compounds of N,N-diethylammonium O,O'-di(p-methoxyphenyl) dithiophosphate in our previous work [14] with the covalence compounds of SBOP-I and SBOP-II in this work, it is clearly that the covalence compounds of SBOP-I and SBOP-II can stable present in HCl solution resulting SBOP-I and SBOP-II will not react with aggressive solution including various ions. This result show that SBOP-I can exhibit the excellent corrosion inhibition of Q235 steel in HCl solution, and further reveal that SBOP-I and SBOP-II all can act as the long-acting corrosion inhibitor.

4. CONCLUSIONS

In conclusion, the corrosion inhibitors of SBOP-I (S-4-methylbenzyl-O,O'-bis(4-nitrophenyl) dithiophosphate) and SBOP-II (S-4-methylbenzyl-O,O'-bis(4-t-butylphenyl)dithio- phosphate) were synthesized and confirmed by elemental analysis, FT-IR, ^{1}H, ^{13}C and ^{31}P NMR in this work. Evaluating the corrosion inhibition of Q235 steel bySBOP-I and SBOP-II in HCl solution found that both SBOP-I and SBOP-II are mixed-type inhibitor, the inhibition efficiency increase with the increase of concentration of inhibitors, decrease with the increasing of HCl concentration and temperature. The adsorption of SBOP-I and SBOP-II on Q235 steel surface obeys Langmuir isotherm, which belongs to chemical adsorption.

ACKNOWLEDGEMENTS

This project is supported financially by the program of Science and Technology Department of Sichuan Province (Nos. 2017JY0180, 2016GZ0172, 2016JY0048, 2016086), the program of Education Department of Sichuan Province (No. 16ZA0358), the project of Dazhou City (No. KJJ2016002), the opening project of Material Corrosion and Protection Key Laboratory of Sichuan Province (No. 2017CL02), the project of Key Laboratories of Fine Chemicals and Surfactants in Sichuan Provincial Universities (No. 2016JXZ03), the project of Zigong Science & Technology and Intellectual Property Bureau (Nos. 2015HX18, 2015CXM01), and the opening project of Key Laboratory of Green Catalysis of Sichuan Institutes of High Education (No. LZJ14201).

References

1. C. Gupta, I. Ahamad, A. Singh, X. H. Xu, Z. P. Sun and Y. H. Lin, *Int. J. Electrochem. Sci.*, 12 (2017) 6379.
2. X. H. Li, S. D. Deng, T. Lin, X. G. Xie and G. B. Du, *Corros. Sci.*, 118 (2017) 202.
3. F. Branzoi and V. Branzoi, *Int. J. Electrochem. Sci.*, 12 (2017) 7638.
4. R. Solmaz, *Corros. Sci.*, 81 (2014) 75.
5. G. Tansuğ, T. Tüken, E.S. Giray, G. Fındıkkıran, G.Sığırcık, O.Demirkol and M. Erbil, *Corros. Sci.*, 81 (2014) 23.
6. C. Lai, H. X.Yang, X.G. Guo, X. L. Su, L. S. Zhou, L. Zhang and B. Xie, *Int. J. Electrochem. Sci.*, 11 (2016) 10462.
7. Y. Guo, M. D. Gao, H. F. Wang and Z. Y. Liu, *Int. J. Electrochem. Sci.*, 12 (2017) 1401.
8. L. Feng, S. T. Zhang, S. Yan, S. Y. Xu and S. J. Chen, *Int. J. Electrochem. Sci.*, 12 (2017) 1915.
9. Shirin Shahabi and Parviz Norouzi, *Int. J. Electrochem. Sci.*, 12 (2017) 2628.

10. A. S. Fouda, M. A. Diab, A.Z. El-Sonbati and S. A. Hassan, *Int. J. Electrochem. Sci.*, 12 (2017) 5072.
11. T. Douadi, H. Hamani, D. Daoud, M. Al-Noaimi and S. Chafaa, *J. Taiwan Ins. Chem. E.*, 71(2017) 388.
12. X. L Su, C. Lai, L.C. Peng, H. Zhu, L.S. Zhou, L. Zhang, X.Q Liu and W. Zhang, *Int. J. Electrochem. Sci.*, 11 (2016) 4828.
13. C. Lai, X. L. Su, T. Jiang, L. S. Zhou, B. Xie, Y. L. and L. K. Zou, *Int. J. Electrochem. Sci.*, 11 (2016) 9413.
14. C. Lai, B. Xie, C. L. Liu, W. Gou, X. L. Su and L. K. Zou, *Int. J. Corros.*, 2016 (2016) 1.
15. Y. Elkhotfi, I. Forsal, E.M. Raki and B. Mernari, *J. Adv. Electrochem.*, 3(2017)141.
16. M. M. Solomon, H. Gerengi, T. Kaya, E. Kaya and S. A. Umoren, *Cellulose*, 24(2017)931.
17. A. Biswas, S. Pal and G. Udayabhanu, *Appl. Surf. Sci.*, 353 (2015) 173.
18. N. Kıcır, G.Tansuğ, M. Erbil and T.Tüken, *Corros. Sci.*, 105 (2016) 88.
19. R. Salghi, S. Jodeh, E. E. Ebenso, H. Lgaz, D. B. Hmamou, I. H. Ali , M. Messali, B. Hammouti and N. Benchat, *Int. J. Electrochem. Sci.*, 12 (2017) 3309.
20. A. Ghames, T. Douadi, S. Issaadi, L. Sibous, K. I. Alaoui, M. Taleb and S.Chafaa, *Int. J. Electrochem. Sci.*, 12 (2017) 4867.
21. X. H. Li, X. G. Xie, S. D. Deng, and G. B. Du, *Corros. Sci.*, 92 (2015) 136.
22. M. Mishra, K. Tiwari, A. K. Singh and V. P. Singh, *Polyhedron*, 77 (2014) 57.
23. P. Singh, A. K. Singh and V. P. Singh, *Polyhedron*, 65 (2013) 73.
24. A. Y. El-Etre, A. H. Tantawy, S. Eid and D. F. Seyam, *J. Basic. Environ. Sci.*, 2 (2017) 128.
25. Y. Lu, C. Lai, X. L. Su, B. Xie, Y. L. Li and N. Chen, *Chem. Res. Appl.*, 29 (2017) 479.
26. J. Wei, B. Xie, L. X. He, Y. L. Li, L. K. Zou and Y. K. Fan, *Chinese. J. Appl. Chem.*, 33(2016) 190.